

## Supplemental data

### **Structural dynamics of the yeast Shwachman-Diamond syndrome protein (Sdo1) on the ribosome and its implication in the 60S subunit maturation**

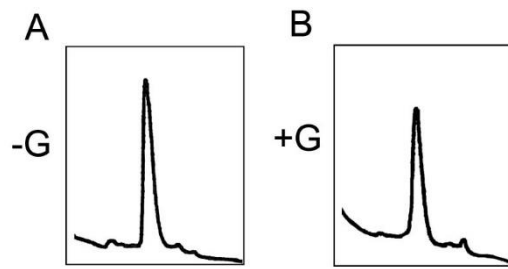
Chengying Ma<sup>1</sup>, Kaige Yan<sup>1</sup>, Dan Tan<sup>2,3</sup>, Ningning Li<sup>1</sup>, Yixiao Zhang<sup>1</sup>, Yi Yuan<sup>1</sup>, Zhifei Li<sup>1</sup>, Meng-Qiu Dong<sup>2,3</sup>, Jianlin Lei<sup>1</sup> and Ning Gao<sup>1,4</sup>

<sup>1</sup>School of Life Sciences, Tsinghua University, Beijing, Beijing 100084, China

<sup>2</sup>National Institute of Biological Sciences, Beijing, Beijing 102206, China

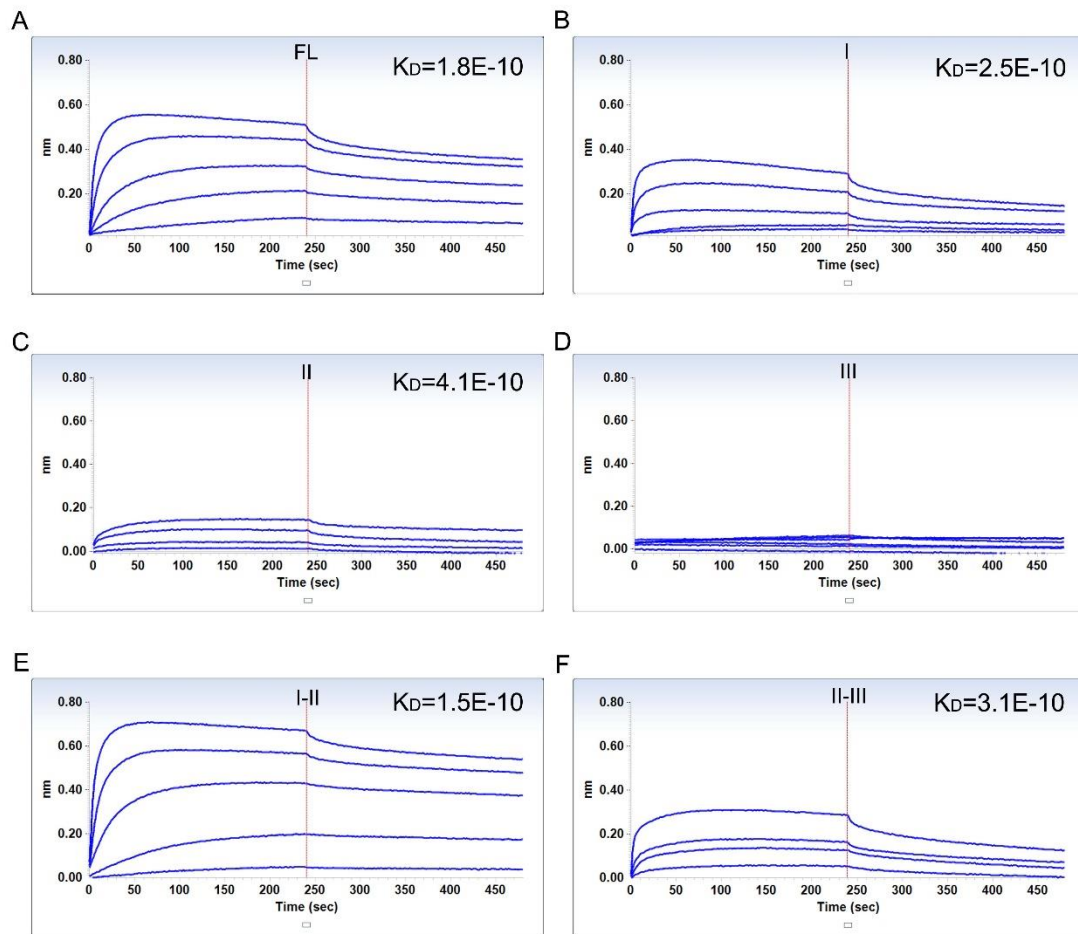
<sup>3</sup>Graduate Program in Chinese Academy of Medical Sciences and Peking Union Medical College, Beijing 100730, China

<sup>4</sup>To whom correspondence may be addressed: School of Life Sciences, Tsinghua University, Beijing 100084, China. Tel: +86-10-62794277; E-mail: [ninggao@tsinghua.edu.cn](mailto:ninggao@tsinghua.edu.cn).



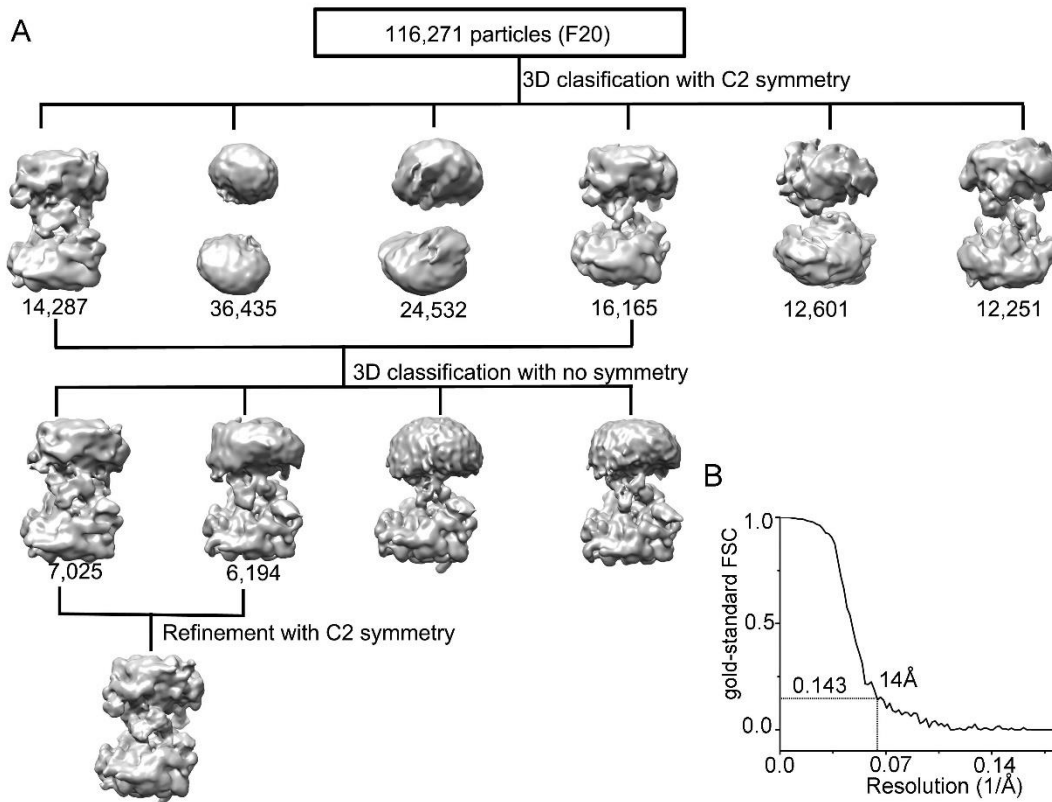
**Supplementary figure S1. 0.1% Glutaraldehyde does not induce 60S dimerization.**

60S subunits were applied to sucrose density gradient centrifugation in the absence (-G) (A) or presence (+G) (B) of 0.1% glutaraldehyde.



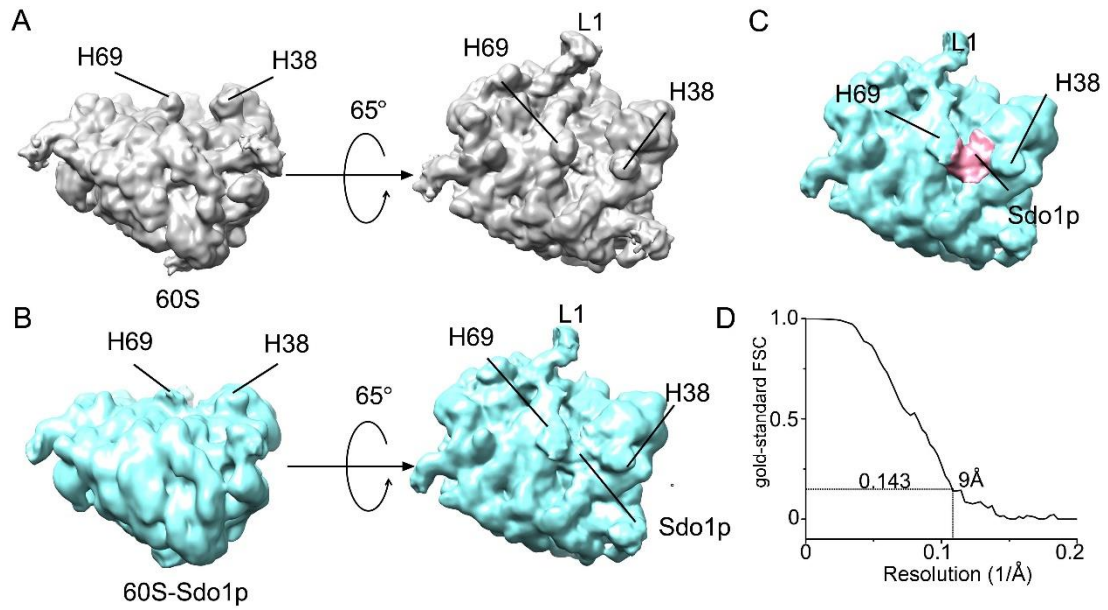
**Supplementary figure S2. Binding of Sdo1p variants to the 60S subunit examined by Bio-layer interferometry.**

(A-F) Global kinetic analysis of the binding of Sdo1p variants to the 60S subunit. Both association (240 sec) and dissociation (240 sec) curves for the binding of FL (full-length), I (domain I), II (domain II), III (domain III), I-II and II-III mutants of Sdo1p to the 60S subunit are shown. Calculated  $K_D$  was also labelled.



### Supplementary figure S3. 3D classification of the dimeric 60S-Sdo1p particles

(A) A total of 116,271 particles were picked and subjected to a cascade of 3D classification. The first round was done with C2-symmetry imposed. Two of the resulting 6 classes were combined and subject to another round of symmetry-free 3D classification. A final dataset (13,219, 11% particles) containing particles from two classes of the second 3D classification was subjected to structural refinement with C2-symmetry imposed. (B) Gold-standard Fourier shell correlation (FSC) curve of the final cryo-EM density map.



**Supplementary figure S4. Structural comparison of the monomeric 60S-Sdo1p complex with the empty 60S subunit.**

(A) Two representative views of the empty 60S subunit. (B) Same as (A), but of the monomeric 60S-Sdo1p complex. (C) Cryo-EM density map of the monomeric 60S-Sdo1p complex, with highlight of the additional density at the ribosomal P-site (red), which could be attributed to Sdo1p (likely domain I). (D) Gold-standard Fourier shell correlation (FSC) curve of the final cryo-EM density map.

